Chinese Journal of Aeronautics, (2014),27(3): 670–677

Chinese Society of Aeronautics and Astronautics
& Beihang University

Chinese Journal of Aeronautics

cja@buaa.edu.cn
www.sciencedirect.com

DOA estimation for attitude determination on communication satellites

Yang Bin [a], He Feng [a], Jin Jin [b], Xiong Huagang [a], Xu Guanghan [a,*]

[a] School of Electronic and Information Engineering, Beihang University, Beijing 100191, China
[b] School of Aerospace, Tsinghua University, Beijing 100084, China

Received 13 May 2013; revised 4 November 2013; accepted 10 December 2013
Available online 24 April 2014

KEYWORDS

Attitude determination;
Communication satellite;
Direction of arrival (DOA) estimation;
Low Earth orbit (LEO);
Smart antennas

Abstract In order to determine an appropriate attitude of three-axis stabilized communication satellites, this paper describes a novel attitude determination method using direction of arrival (DOA) estimation of a ground signal source. It differs from optical measurement, magnetic field measurement, inertial measurement, and global positioning system (GPS) attitude determination. The proposed method is characterized by taking the ground signal source as the attitude reference and acquiring attitude information from DOA estimation. Firstly, an attitude measurement equation with DOA estimation is derived in detail. Then, the error of the measurement equation is analyzed. Finally, an attitude determination algorithm is presented using a dynamic model, the attitude measurement equation, and measurement errors. A developing low Earth orbit (LEO) satellite which tests mobile communication technology with smart antennas can be stabilized in three axes by corporately using a magnetometer, reaction wheels, and three-axis magnetorquer rods. Based on the communication satellite, simulation results demonstrate the effectiveness of the method. The method could be a backup of attitude determination to prevent a system failure on the satellite. Its precision depends on the number of snapshots and the input signal-to-noise ratio (SNR) with DOA estimation.

1. Introduction

Attitude of communication satellites, which should be as accurate as possible to obtain a better data link, is determined by measurements from attitude sensors.[1–3] Attitude sensors output the projection of the reference vector in the sensitive direction of attitude.[3–5] Commonly used vectors are defined by stars, the Sun, the Earth, geomagnetic field, inertial space, and GPS satellites.[3–6] Owing to distinguishing features of the above sensors, most of communication satellites achieve attitude determination by corporately using different attitude references to prevent a system failure.[1,2] For example, a three-axis gyroscope, a three-axis magnetometer, and a coarse horizon sensor are used for attitude references of Iridium satellites.[1] The attitude of Globalstar satellites is determined by four Sun sensors, a horizon sensor, a three-axis magnetometer, and GPS.[2]

* Corresponding author. Tel.: +86 10 62802002.
E-mail address: guanghanxu@hotmail.com (G. Xu).

Peer review under responsibility of Editorial Committee of CJA.

ELSEVIER Production and hosting by Elsevier

http://dx.doi.org/10.1016/j.cja.2014.04.010

The work in this paper is based on a developing low Earth orbit (LEO) satellite, which tests mobile communication technology with fixed smart antennas. The transient space information between a ground signal source and the smart antennas can be obtained by array signal processing. The direction of arrival (DOA) estimation uses the data received by the smart array to estimate the direction of the signal source.[7,8] At present, DOA estimation algorithms have been applied in direction estimation of signal sources.[9–12] A new method of attitude estimation using a dipole triad antenna on an aircraft was reported in Ref. 13. The attitude angle of the aircraft can be determined by corporately using DOA estimation of a ground source and an electric ellipse orientation angle in Ref. 13. However, the method is base on a dipole triad antenna on an aircraft, not on smart antennas. The DOA of a ground signal has never been used in the attitude determination on communication satellites. The DOA contains attitude information of smart antennas relative to a ground signal source. Therefore, the ground signal source of a known location can be used for extra attitude reference of a satellite.

This paper is interested in using the DOA estimation of a ground signal source (a ground station or a ground mobile user) as the observation of the extended Kalman filter (EKF) for attitude determination of a communication satellite. A DOA attitude measurement equation is derived on the basis of the ground signal source location, the satellite orbit position, and the space geometric information between the signal source and the smart antennas. The error of the attitude measurement equation with DOA is analyzed in detail. Then, an attitude determination algorithm is presented using the dynamics of the satellite, the attitude measurement equation with DOA estimation, and the measurement errors. Finally, the proposed method of attitude determination is analyzed in terms of stability, convergence time, and estimation accuracy by exploring the influences of the number of snapshots and input signal-to-noise ratio (SNR).

This paper is organized as follows. The basic model of satellite attitude is introduced in Section 2. The deduction steps of attitude measurement with DOA estimation are presented in Section 3. The error of the attitude measurement equation with DOA is analyzed in Section 4. The attitude determination algorithm with DOA is derived in Section 5. Simulation results of the method are shown and analyzed in Section 6. Conclusions and future work are put forward in Section 7.

2. Basic model

To address the attitude determination problem of a satellite with smart antennas, Fig. 1 shows the relation between the satellite and the attitude reference of the ground signal source S_d. In this paper, we only consider the case of a single ground source for attitude determination, and assume that a line-of-sight (LOS) signal component from the ground to the satellite is available at the smart antennas.

Three reference frames are illustrated in Fig. 1, all being right-hand orthogonal triads. The orbital frame $O\eta\xi\zeta$ is denoted as F_o, where O is the mass center of the satellite, ζ axis points to the center of the Earth, and η axis points along the flight direction. The satellite body fixed frame is denoted as F_b, and the receiving smart antennas frame $Rxyz$ is denoted as F_r, where x axis is parallel to x' body axis and y to y' body axis, and R is the center of the smart antennas which is located in the x–y plane.

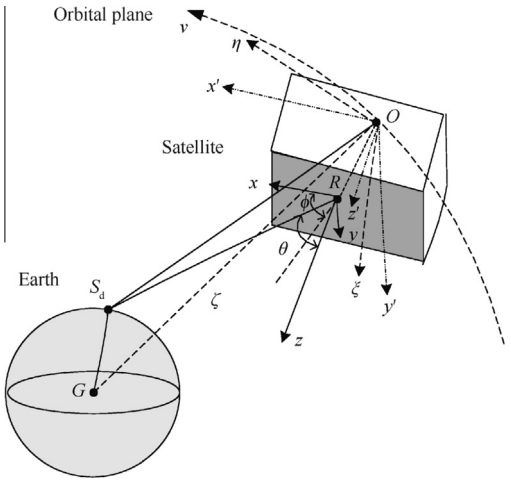

Fig. 1 DOA and attitude of reference frames for the communication satellite.

In Fig. 1, the DOA vector is defined by (θ, ϕ) in F_r, where θ is the polar angle which is measured from the signal source vector $\boldsymbol{v}_{RS_d}$ to z axis, and ϕ is the azimuth angle that corresponds to θ in the same spherical coordinate system. Then, the unit vector of the reference vector $\boldsymbol{v}_{RS_d}$ denoted as $\boldsymbol{S}_{dr} = [S^r_{dx},\ S^r_{dy},\ S^r_{dz}]^T$ in F_r is calculated as

$$\boldsymbol{S}_{dr} = [\sin\theta\cos\phi, \sin\theta\sin\phi, \cos\theta]^T \tag{1}$$

The satellite attitude is defined by the orientation of the satellite body fixed frame F_b with respect to the orbital frame F_o. The attitude matrix $\boldsymbol{C}_{bo}$ is defined as the transfer matrix from F_o to F_b and $\boldsymbol{C}_{ob} = \boldsymbol{C}^T_{bo}$ is the attitude matrix from F_b to F_o. Since the smart antennas frame F_r parallels to F_b, the attitude matrix $\boldsymbol{C}_{ro}$ from F_o to F_r is given by

$$\boldsymbol{C}_{ro} = \boldsymbol{C}_{bo} \tag{2}$$

The attitude from F_o to F_b is described by quaternion parameterization

$$\dot{\boldsymbol{q}}_{bo} = [q_{bo_0}, \boldsymbol{q}_{bo}] \tag{3}$$

with

$$q_{bo} = [q_{bo_1}, q_{bo_2}, q_{bo_3}]^T \tag{4}$$

The quaternion satisfies the following normalization constraint

$$\boldsymbol{q}^2_{bo_0} + q^2_{bo_1} + q^2_{bo_2} + q^2_{bo_3} = 1 \tag{5}$$

$\boldsymbol{C}_{bo}$ can be obtained by

$$\boldsymbol{C}_{bo} = \left(q^2_{bo_0} - \boldsymbol{q}^T_{bo}\boldsymbol{q}_{bo}\right)\boldsymbol{E}_{3\times3} + 2\boldsymbol{q}_{bo}\boldsymbol{q}^T_{bo} - 2q_{bo_0}[\boldsymbol{q}_{bo}\times] \tag{6}$$

where $\boldsymbol{E}_{3\times3}$ is the identity matrix and $[\boldsymbol{q}_{bo}\times]$ is the cross-product matrix of the vector $\boldsymbol{q}_{bo}$, which is defined by

$$[\boldsymbol{q}_{bo}\times] = \begin{bmatrix} 0 & -q_{bo_3} & q_{bo_2} \\ q_{bo_3} & 0 & -q_{bo_1} \\ -q_{bo_2} & q_{bo_1} & 0 \end{bmatrix} \tag{7}$$

3. Attitude measurement equation with DOA

3.1. Basic model of DOA estimation

The DOA estimation is based on the relative arrival times of a source signal at the array elements and the second-order statistics.[7,9] Assume that there are M elements in the antenna array located at the $x-y$ plane. A steering vector $\boldsymbol{a}(\theta,\phi)$ characterizes the relative phase with the DOA (θ,ϕ). The received input data vector $\boldsymbol{X}(t)=[x_1(t),x_2(t),\ldots,x_M(t)]^{\mathrm{T}}$ can be expressed as

$$\boldsymbol{X}(t)=\boldsymbol{a}(\theta,\phi)s(t)+\boldsymbol{N}(t) \tag{8}$$

where $s(t)$ is the received signal and $\boldsymbol{N}(t)=[n_1(t),n_2(t),\ldots,n_M(t)]^{\mathrm{T}}$ is the noise vector. The spatial covariance matrix $\boldsymbol{R}_{xx}$ is defined in

$$\boldsymbol{R}_{xx}=E\left[\boldsymbol{X}(t)\boldsymbol{X}(t)^{\mathrm{H}}\right] \tag{9}$$

where $\boldsymbol{X}(t)^{\mathrm{H}}$ is the complex conjugate transpose of $\boldsymbol{X}(t)$.[9] In practice, this matrix is estimated by L snapshots of the actual antenna array output, as shown in

$$\boldsymbol{R}_{xx}\approx\frac{1}{L}\sum_{l=1}^{L}\boldsymbol{X}(lT)\boldsymbol{X}(lT)^{\mathrm{H}} \tag{10}$$

where T is the sampling interval.[9]

An eigenvalue decomposition of $\boldsymbol{R}_{xx}$ can be used to form a noise subspace matrix $\boldsymbol{V}_M$ containing the noise eigenvectors.[7,9] Multiple signal classification (MUSIC) is a high-resolution estimation method of DOA using the steering vector.[7,14,15] The DOA $(\hat{\theta},\hat{\phi})$ of the signal can be estimated by locating the peaks of an MUSIC spatial spectrum[14]

$$P_{\mathrm{MUSIC}}(\theta,\phi)=1/\boldsymbol{a}^{\mathrm{H}}(\theta,\phi)\boldsymbol{V}_M\boldsymbol{V}_M^{\mathrm{H}}\boldsymbol{a}(\theta,\phi) \tag{11}$$

The precision of the DOA $(\hat{\theta},\hat{\phi})$ is limited by the input SNR and the number of snapshots on condition that the difference between the elements and the mutual coupling between the antennas array are compensated.[9,16,17]

Using the DOA $(\hat{\theta},\hat{\phi})$ estimated from Eq. (11), the estimated unit vector $\hat{\boldsymbol{S}}_{\mathrm{dr}}$ is written as

$$\hat{\boldsymbol{S}}_{\mathrm{dr}}=[\sin\hat{\theta}\cos\hat{\phi},\sin\hat{\theta}\sin\hat{\phi},\cos\hat{\theta}]^{\mathrm{T}}=\boldsymbol{S}_{\mathrm{dr}}+\boldsymbol{W} \tag{12}$$

where $\boldsymbol{W}=[W_x,W_y,W_z]^{\mathrm{T}}$ is the error vector of reference vector estimation in F_{r}, which depends on the DOA $(\hat{\theta},\hat{\phi})$.

3.2. Attitude measurement equation with DOA

In the on-board system, the satellite location vector $\boldsymbol{v}_{OG}$ denoted as $\boldsymbol{G}_{\mathrm{o}}=\left[G_\eta^{\mathrm{o}},G_\xi^{\mathrm{o}},G_\zeta^{\mathrm{o}}\right]^{\mathrm{T}}$ can be calculated from the orbit position in F_{o}. Since the location information of the ground signal source is uploaded by the uplink with the smart antennas, the ground signal source vector $\boldsymbol{v}_{S_{\mathrm{d}}G}$ denoted as $\boldsymbol{S}_{\mathrm{do}}=\left[S_{d\eta}^{\mathrm{o}},S_{d\xi}^{\mathrm{o}},S_{d\zeta}^{\mathrm{o}}\right]^{\mathrm{T}}$ in F_{o} is known in the on-board system. The vector $v_{OS_{\mathrm{d}}}$, which is the direction from the satellite to the ground signal source, denoted as $\boldsymbol{D}_{\mathrm{o}}=\left[D_\eta^{\mathrm{o}},D_\xi^{\mathrm{o}},D_\zeta^{\mathrm{o}}\right]^{\mathrm{T}}$ in F_{o} is then given by

$$\boldsymbol{D}_{\mathrm{o}}=\boldsymbol{G}_{\mathrm{o}}-\boldsymbol{S}_{\mathrm{do}} \tag{13}$$

Moreover, the vector $\boldsymbol{v}_{OR}$, which is the direction from the satellite's mass point to the center of the smart antennas, denoted as $\boldsymbol{R}_{\mathrm{b}}=[R_{x'}^{\mathrm{b}},R_{y'}^{\mathrm{b}},R_{z'}^{\mathrm{b}}]^{\mathrm{T}}$ is known in F_{b}. Therefore, $\boldsymbol{v}_{OR}$ denoted as $\boldsymbol{R}_{\mathrm{o}}=\left[R_\eta^{\mathrm{o}},R_\xi^{\mathrm{o}},R_\zeta^{\mathrm{o}}\right]^{\mathrm{T}}$ in F_{o} is calculated as

$$\boldsymbol{R}_{\mathrm{o}}=\boldsymbol{C}_{\mathrm{bo}}^{\mathrm{T}}\boldsymbol{R}_{\mathrm{b}} \tag{14}$$

The unit vector $\boldsymbol{v}_{RS_{\mathrm{d}}}$ denoted as $\boldsymbol{S}_{\mathrm{o}}=\left[S_\eta^o,S_\xi^o,S_\zeta^o\right]$ in F_{o} is calculated as

$$\boldsymbol{S}_{\mathrm{o}}=\frac{\boldsymbol{D}_{\mathrm{o}}-\boldsymbol{R}_{\mathrm{o}}}{\|\boldsymbol{D}_{\mathrm{o}}-\boldsymbol{R}_{\mathrm{o}}\|} \tag{15}$$

Using Eq. (2), in the smart antennas frame F_{r}, $\boldsymbol{S}_{\mathrm{dr}}$ can be given by

$$\boldsymbol{S}_{\mathrm{dr}}=\boldsymbol{C}_{\mathrm{ro}}\boldsymbol{S}_{\mathrm{o}}=\boldsymbol{C}_{\mathrm{bo}}\boldsymbol{S}_{\mathrm{o}} \tag{16}$$

Compared with the altitude of the satellite and the location of the ground signal source, the satellite size could be treated as infinitesimal (i.e., $\|\boldsymbol{R}_{\mathrm{b}}\|\ll\|\boldsymbol{D}_{\mathrm{o}}\|$). Then, using Eqs. (13)–(15), $\boldsymbol{S}_{\mathrm{o}}$ can be rewritten as

$$\boldsymbol{S}_{\mathrm{o}}\approx\frac{\boldsymbol{G}_{\mathrm{o}}-\boldsymbol{S}_{\mathrm{do}}}{\|\boldsymbol{G}_{\mathrm{o}}-\boldsymbol{S}_{\mathrm{do}}\|} \tag{17}$$

Therefore, using Eqs. (12) and (16), and the approximation above, the attitude measurement equation with DOA estimation is determined as

$$[\sin\hat{\theta}\cos\hat{\phi},\sin\hat{\theta}\sin\hat{\phi},\cos\hat{\theta}]^{\mathrm{T}}\approx\boldsymbol{C}_{\mathrm{bo}}\frac{\boldsymbol{G}_{\mathrm{o}}-\boldsymbol{S}_{\mathrm{do}}}{\|\boldsymbol{G}_{\mathrm{o}}-\boldsymbol{S}_{\mathrm{do}}\|}+\boldsymbol{W} \tag{18}$$

4. Error analysis of attitude measurement

4.1. Smart antennas model

In our study, the LEO satellite we are developing will run in a Sun-synchronous circular orbit with an altitude of 800 km and a local time of descending node of nominal 8:00 AM.[18] The LEO satellite tests mobile communication technology with a uniform circular array (UCA) which is composed of 12 quadrifilar helix antennas (QHAs). The uplink signal wavelength is $\lambda=150$ mm. Fig. 2 represents the smart antennas model of the satellite.

In Fig. 2, the UCA radius is $r=150$ mm. d and d_m are the distance from the signal source S_{d} to center of array R and the

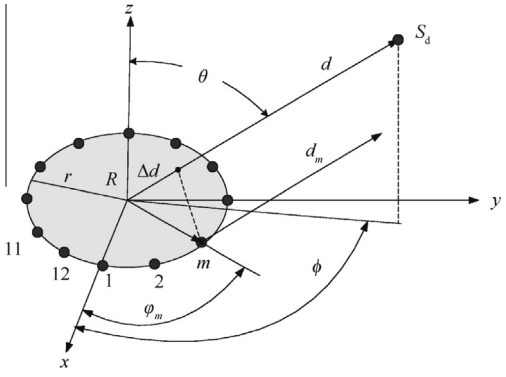

Fig. 2 Smart antennas model.

element. The element phase angle is $\varphi_m = 2\pi(m-1)/12$ for $m = 1, 2, \ldots, 12$. The unit vector of $\boldsymbol{v}_{Rm}$ denoted as $\boldsymbol{M}_{\mathrm{r}} = \left[M_x^{\mathrm{r}}, M_y^{\mathrm{r}}, M_z^{\mathrm{r}}\right]^{\mathrm{T}}$ in F_{r} is given by

$$\boldsymbol{M}_{\mathrm{r}} = [\cos\varphi_m, \sin\varphi_m, 0]^{\mathrm{T}} \tag{19}$$

Using Eqs. (1) and (19), the distance difference between different locations from far-field electromagnetic wave Δd is given by

$$\Delta d = d - d_m = r\boldsymbol{S}_{\mathrm{dr}}\boldsymbol{M}_{\mathrm{r}} = r\sin\theta\cos(\phi - \varphi_m) \tag{20}$$

The difference between the elements and the mutual coupling of the antenna array can be compensated by array calibration methods.[9,16,17] From this, the steering vector is given by

$$\boldsymbol{a}(\theta,\phi) = \begin{bmatrix} \exp\left(\mathrm{j}\dfrac{2\pi}{\lambda} r\sin\theta\cos\left(\phi - \dfrac{2\pi}{12}\cdot 0\right)\right) \\ \exp\left(\mathrm{j}\dfrac{2\pi}{\lambda} r\sin\theta\cos\left(\phi - \dfrac{2\pi}{12}\cdot 1\right)\right) \\ \vdots \\ \exp\left(\mathrm{j}\dfrac{2\pi}{\lambda} r\sin\theta\cos\left(\phi - \dfrac{2\pi}{12}\cdot 11\right)\right) \end{bmatrix} \tag{21}$$

4.2. Error analysis

Regarding to the satellite orbit and smart antennas model, we use an orbital simulation package to generate 8 ground stations. The minimum elevation angle for ground stations is 10 degrees (i.e., $0^\circ \leqslant \theta \leqslant 62^\circ, 0^\circ \leqslant \phi \leqslant 360^\circ$). In addition, at least one ground signal is available at the smart antennas for 3000 s orbit plane time in this simulation. In the simulation case, the ground station informs the satellite to prepare to hand off because it knows both the station's location and the satellite's location. The online processing step size of the satellite is 250 ms. Using Eqs. (11) and (21), the results of the DOA $(\hat{\theta}, \hat{\phi})$ are given. Figs. 3 and 4 show the theoretical values of the DOA (θ, ϕ) and the DOA $(\hat{\theta}, \hat{\phi})$ in terms of the number of snapshots L and the input SNR.

It is seen that the precision of the DOA $(\hat{\theta}, \hat{\phi})$ is limited by the number of snapshots and the input SNR. In addition, the DOA $(\hat{\theta}, \hat{\phi})$ can be more accurate as the increases of the number of snapshots and the input SNR. After that, the statistical properties analysis of $\boldsymbol{W}$ is plotted in Fig. 5 using Eq. (12).

As can be seen in Fig. 5, the noise vector $\boldsymbol{W}$ is independent and an identically distributed Gaussian random process with zero-mean. In addition, the variance of $\boldsymbol{W}$ becomes bigger with the decreases of the number of snapshots and the input SNR. Then, the covariance $\boldsymbol{R}_{\boldsymbol{W}}$ of $\boldsymbol{W}$ can be chosen as follows:

$$\boldsymbol{R}_{\boldsymbol{W}} = \begin{bmatrix} \sigma_{W_x}^2 & 0 & 0 \\ 0 & \sigma_{W_y}^2 & 0 \\ 0 & 0 & \sigma_{W_z}^2 \end{bmatrix} \tag{22}$$

where $\sigma_{W_x}^2$, $\sigma_{W_y}^2$, and $\sigma_{W_z}^2$ are the variances of x axis, y axis, and z axis, respectively, which can be calculated with the above simulations.

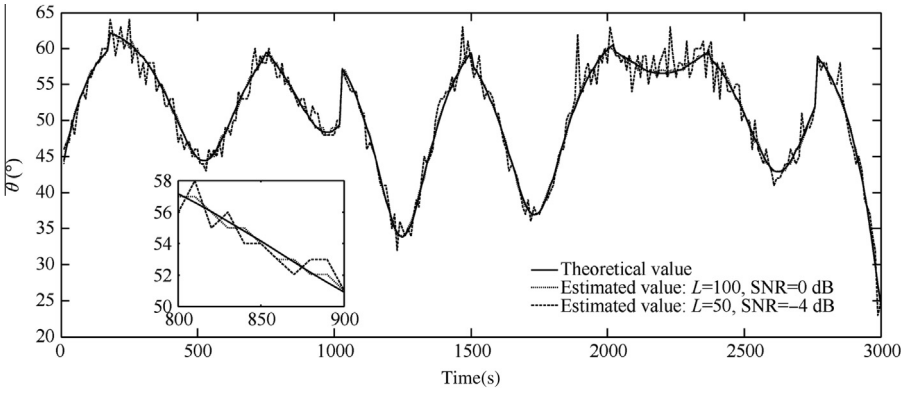

Fig. 3 $\hat{\theta}$ of the DOA estimation.

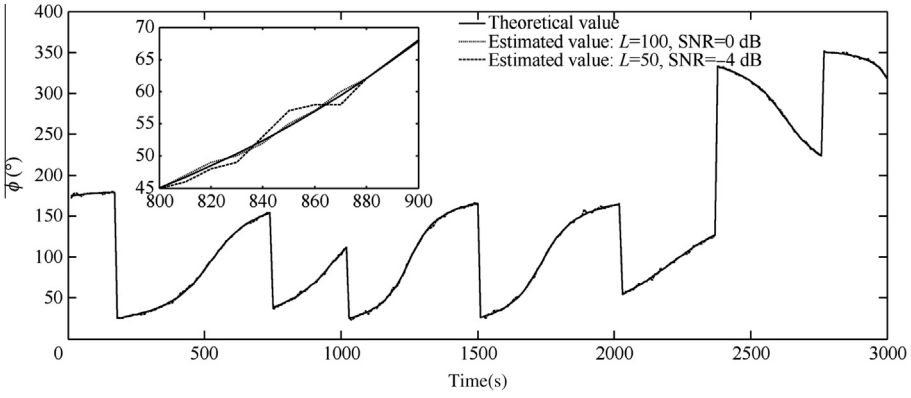

Fig. 4 $\hat{\phi}$ of the DOA estimation.

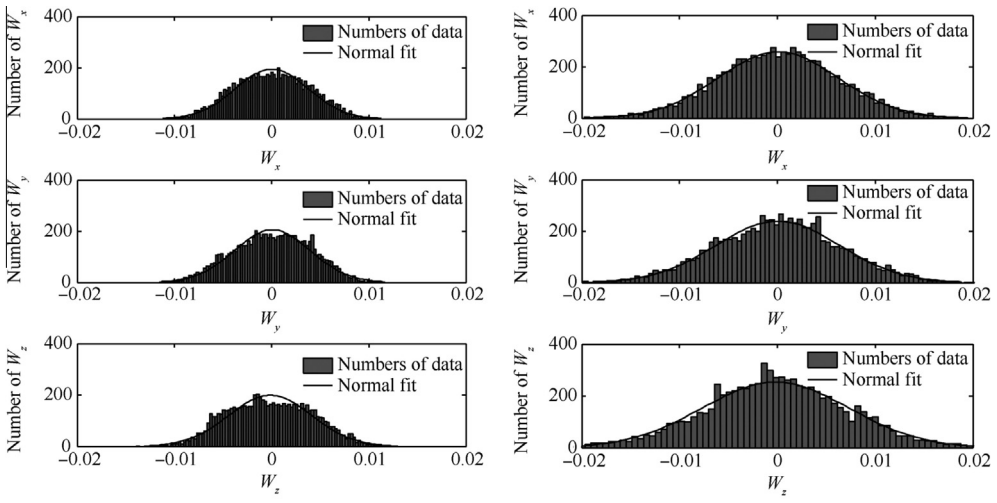

(a) L=100, SNR=0 dB (b) L=50, SNR=−4 dB

Fig. 5 Statistical properties analysis of $\boldsymbol{W}$.

5. Attitude determination algorithm

5.1. The satellite dynamic model

The satellite can be stabilized in three axes by corporately using reaction wheels and three-axis magnetorquer rods.[18] Therefore, the dynamic equation is given by

$$\boldsymbol{I}_{3\times3}\dot{\boldsymbol{\omega}}_{\mathrm{bi}}(t) = -(\boldsymbol{\omega}_{\mathrm{bi}}(t)\times)(\boldsymbol{I}_{3\times3}\boldsymbol{\omega}_{\mathrm{bi}}(t)+\boldsymbol{h}(t)) - \dot{\boldsymbol{h}}(t) + \boldsymbol{T}_{\mathrm{mt}}(t) + \boldsymbol{T}_{\mathrm{d}}(t) \tag{23}$$

and

$$\boldsymbol{\omega}_{\mathrm{bo}} = \boldsymbol{\omega}_{\mathrm{bi}} - \mathbf{C}_{\mathrm{bo}}\boldsymbol{\omega}_{\mathrm{o}} \tag{24}$$

where $\boldsymbol{\omega}_{\mathrm{bi}}$ is the inertial referenced angular velocity vector; $\boldsymbol{h}$ is the total angular momentum of wheels; $\boldsymbol{T}_{\mathrm{mt}}$ is the torque produced by magnetorquer rods, $\boldsymbol{T}_{\mathrm{d}}$ is the disturbance torques; $\boldsymbol{\omega}_{\mathrm{bo}}$ is the attitude angular rate in F_{o}; $\boldsymbol{\omega}_{\mathrm{o}}$ is the satellite orbit angular rate; $\boldsymbol{I}_{3\times3}$ is the inertia matrix of the satellite defined by

$$\boldsymbol{I}_{3\times3} = \begin{bmatrix} 6.6199 & 0.01636 & 0.2363 \\ 0.01636 & 8.95 & 0.2247 \\ 0.2363 & 0.2247 & 9.4968 \end{bmatrix} \ \mathrm{kg}\cdot\mathrm{m}^2 \tag{25}$$

5.2. EKF algorithm

The EKF algorithm is employed to determine the attitude using the DOA information of the ground signal during the three-axis stabilized phase of the satellite, and the estimation state vector contains six elements

$$\boldsymbol{x}(k) = \left[\boldsymbol{\omega}_{\mathrm{bi}}^{\mathrm{T}}(k), \boldsymbol{q}_{\mathrm{bo}}^{\mathrm{T}}(k)\right]^{\mathrm{T}} \tag{26}$$

Then, using Eqs. (6), (23) and (24), the state dynamic equation is given by

$$\begin{bmatrix}\dot{\boldsymbol{\omega}}_{\mathrm{bi}}(t)\\ \dot{\boldsymbol{q}}_{\mathrm{bo}}(t)\end{bmatrix} = f\left(\begin{bmatrix}\boldsymbol{\omega}_{\mathrm{bi}}(t)\\ \boldsymbol{q}_{\mathrm{bo}}(t)\end{bmatrix}\right) = \begin{bmatrix} \boldsymbol{I}_{3\times3}^{-1}\{-\boldsymbol{\omega}_{\mathrm{bi}}(t)\times[\boldsymbol{I}_{3\times3}\boldsymbol{\omega}_{\mathrm{bi}}(t)+\boldsymbol{h}(t)] - [\boldsymbol{h}(t)-\boldsymbol{h}(t-\Delta t)]/\Delta t + \boldsymbol{T}_{\mathrm{d}}(t) + \boldsymbol{T}_{\mathrm{mt}}(t)\} \\ \frac{1}{2}\{q_{\mathrm{bo}_0}(t)\boldsymbol{E}_{3\times3} + [\boldsymbol{q}_{\mathrm{bo}}(t)]\times\}[\boldsymbol{\omega}_{\mathrm{bi}}(t) - \boldsymbol{C}_{\mathrm{bo}}(t)\boldsymbol{\omega}_{\mathrm{o}}(t)] \end{bmatrix} \tag{27}$$

The EKF is widely used to estimate state variables with the state dynamic equation and the attitude measurement equation.[19,20] The state dynamic equation Eq. (27) is expanded as the first-order Taylor series about the estimate $\hat{\boldsymbol{x}}(k/k)$ using the EKF algorithm.[18–20] Therefore, the transition matrix of Eq. (27) denoted as $\boldsymbol{\Phi}(k)$ is given by

$$\boldsymbol{\Phi}(k+1/k) \approx \boldsymbol{E}_{6\times6} + \boldsymbol{A}\Delta t \tag{28}$$

where $\Delta t = 250$ ms is the step size of the discretization on the communication satellite and $\boldsymbol{A}$ is calculated as

$$\boldsymbol{A} = \begin{bmatrix} \boldsymbol{I}_{3\times3}^{-1}\{[(\boldsymbol{I}\boldsymbol{\omega}_{\mathrm{bi}}(k/k)+\boldsymbol{h}(k))\times] - [\boldsymbol{\omega}_{\mathrm{bi}}(k/k)\times]\boldsymbol{I}_{3\times3}\} & \boldsymbol{0}_{3\times3} \\ 0.5\boldsymbol{E}_{3\times3} & -[\boldsymbol{\omega}_{\mathrm{bi}}(k/k)\times] \end{bmatrix} \tag{29}$$

The noise of the state dynamic equation is uncorrelated observation noise with covariance $\boldsymbol{Q} = 10^{-9}\boldsymbol{E}_{6\times6}$, due to the disturbance torque and linearization error of the state dynamic equation Eq. (27).[18]

In addition, using Eqs. (16) and (26), the attitude measurement equation Eq. (18) can be rewritten as

$$[\sin\hat{\theta}\cos\hat{\phi}, \sin\hat{\theta}\sin\hat{\phi}, \cos\hat{\theta}]^{\mathrm{T}} = \boldsymbol{S}_{\mathrm{dr}}\left(\begin{bmatrix}\boldsymbol{\omega}_{\mathrm{bi}}(t)\\ \boldsymbol{q}_{\mathrm{bo}}(t)\end{bmatrix}\right) + \boldsymbol{W} \tag{30}$$

In a similar process of the state dynamic equation, the attitude measurement equation Eq. (30) is expanded about $\hat{\boldsymbol{x}}(k+1/k)$ and is truncated at the first order. Thus, using Eqs. (6) and (7), the measurement matrix denoted as $\boldsymbol{H}(k+1)$ is given by

$$\boldsymbol{H}(k+1)=\left.\frac{\partial \boldsymbol{S}_{\mathrm{dr}}}{\partial \boldsymbol{x}^{\mathrm{T}}}\right|_{\boldsymbol{x}=\hat{\boldsymbol{x}}(k+1/k)}=\left[\begin{bmatrix}\frac{\partial}{\partial\hat{\boldsymbol{\omega}}^{\mathrm{T}}(k+1/k)}\boldsymbol{S}_{\mathrm{dr}}(k+1)\end{bmatrix}^{\mathrm{T}}\begin{bmatrix}\frac{\partial}{\partial\hat{\boldsymbol{q}}_{\mathrm{bo}}^{\mathrm{T}}(k+1/k)}\boldsymbol{S}_{\mathrm{dr}}(k+1)\end{bmatrix}^{\mathrm{T}}\right]^{\mathrm{T}} \tag{31}$$

where

$$\frac{\partial}{\partial\hat{\boldsymbol{\omega}}^{\mathrm{T}}(k+1/k)}\boldsymbol{S}_{\mathrm{dr}}(k+1)=\boldsymbol{0}_{3\times3} \tag{32}$$

and

$$\begin{aligned}\frac{\partial}{\partial\hat{\boldsymbol{q}}_{\mathrm{bo}}^{\mathrm{T}}(k+1/k)}\boldsymbol{S}_{\mathrm{dr}}(k+1)&\approx\lim_{\Delta\boldsymbol{q}_{\mathrm{bo}}^{\mathrm{T}}\to0}\frac{[2\hat{\boldsymbol{S}}_{\mathrm{dr}}(k+1/k)\times]\Delta\boldsymbol{q}_{\mathrm{bo}}}{\Delta\boldsymbol{q}_{\mathrm{bo}}^{T}}\\&=2\left[\left(\hat{\boldsymbol{C}}_{\mathrm{bo}}(k+1/k)\frac{\boldsymbol{G}_{\mathrm{o}}(k+1)-\boldsymbol{S}_{\mathrm{do}}(k+1)}{\|\boldsymbol{G}_{\mathrm{o}}(k+1)-\boldsymbol{S}_{\mathrm{do}}(k+1)\|}\right)\times\right]\end{aligned} \tag{33}$$

6. Simulation results

In this section, two simulations are presented: (1) the attitude determination with DOA is simulated first to show the efficiency of the proposed method; (2) the Monte Carlo simulation is then presented to show the influences of the input SNR and the number of snapshots. The flight missions in those simulations are the same as the case in Section 4.2 and at least one ground signal is available at the satellite for 5000 s orbit plane time. The initial Euler angles are yaw = 50°, roll = 50°, and pitch = 50°, and the initial inertial referenced angular velocity $\boldsymbol{\omega}_{\mathrm{bi}}$ is $[0.5, 0.5, 0.5]^{\mathrm{T}}(^\circ)$/s. In addition, $\boldsymbol{R}_{\boldsymbol{W}}$ and $\boldsymbol{Q}$ are chosen the same as in Sections 4.2 and 5.2.

The first simulation considers that the number of snapshots is $L = 100$ and the input SNR is 0 dB. The total simulation time is about 5000 s (one orbit cycle). Figs. 6 and 7 depict the estimated results of the Euler angles and the inertial referenced angular velocity $\boldsymbol{\omega}_{\mathrm{bi}}$ using the DOA estimation in this simulation case. Simulation results show that the errors of the attitude angles converge to a value of 0.5° within 1500 s and the errors of the angular velocity take almost 1000 s to reach 0.1(°)/s. It is acceptable in the Earth pointing estimation accuracy of the communication satellite. In addition, the period for observation of each station or mobile user is about 10 min (i.e., 600 s) for the LEO satellite. Therefore, the method is available on condition that at least 3 ground stations or

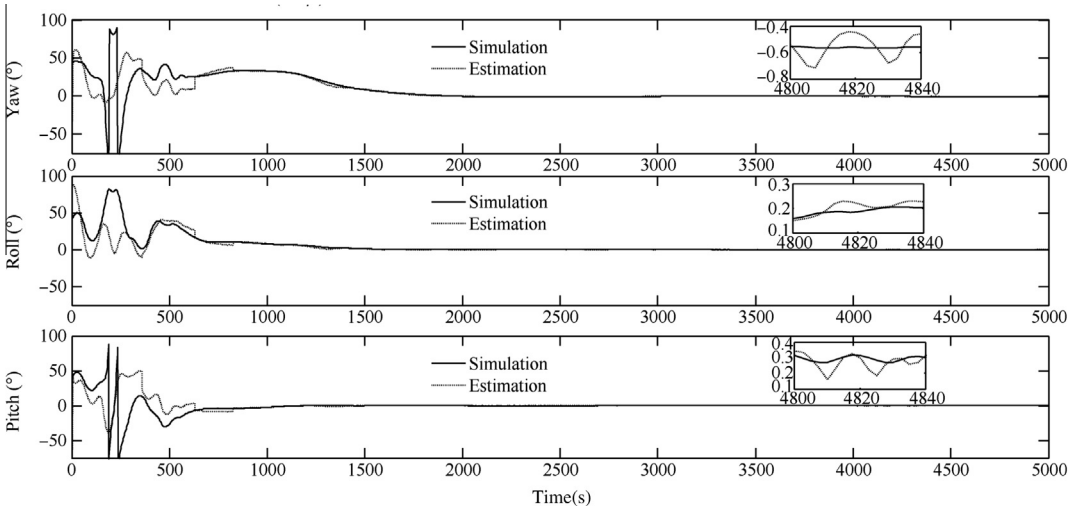

Fig. 6 Estimation errors of attitude angles.

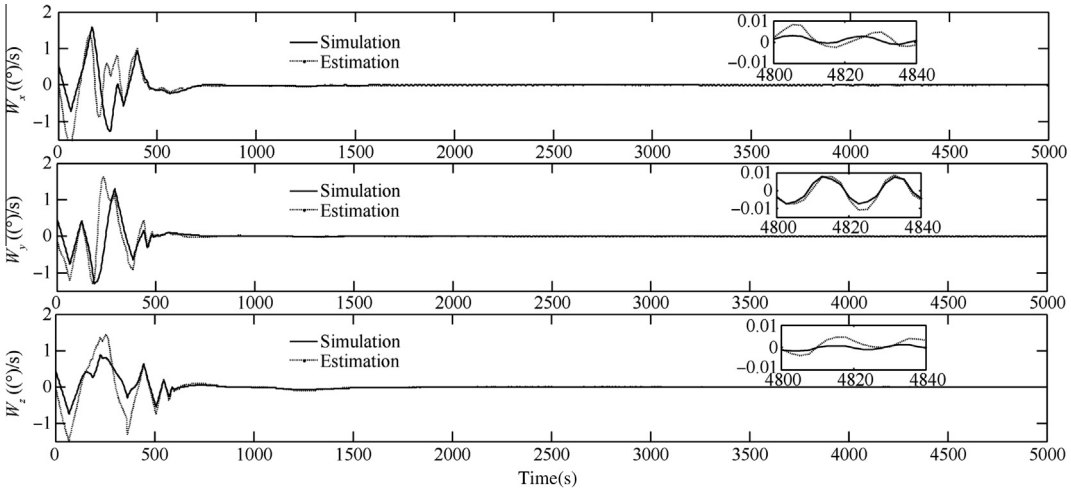

Fig. 7 Estimation errors of angular velocity.

Table 1 RMSE of the attitude determination versus the input SNR.

Number of snapshots	SNR (dB)	RMSE of $\hat{\theta}$ (°)	RMSE of $\hat{\phi}$ (°)	RMSE of yaw (°)	RMSE of roll (°)	RMSE of pitch (°)
100	−14	11.118	68.128	7.397	3.662	1.732
100	−12	4.106	17.337	0.652	0.177	0.457
100	−10	1.518	1.307	0.130	0.079	0.215
100	−8	0.921	0.791	0.109	0.078	0.157
100	−6	0.595	0.534	0.094	0.071	0.111
100	−2	0.354	0.334	0.084	0.060	0.094
100	0	0.315	0.308	0.083	0.061	0.094
100	14	0.287	0.289	0.084	0.060	0.093

Table 2 RMSE of the attitude determination versus the number of snapshots.

Number of snapshots	SNR (dB)	RMSE of $\hat{\theta}$ (°)	RMSE of $\hat{\phi}$ (°)	RMSE of yaw (°)	RMSE of roll (°)	RMSE of pitch (°)
1	0	8.354	51.089	15.956	10.071	6.852
10	0	0.781	0.684	0.099	0.070	0.146
20	0	0.408	0.385	0.086	0.064	0.100
50	0	0.342	0.326	0.084	0.062	0.091
100	0	0.315	0.308	0.083	0.061	0.094
1000	0	0.287	0.289	0.084	0.062	0.093

mobile users continuously communicate with the satellite for an attitude determination which needs 1500 s for the convergence. The results demonstrate that the proposed method using the DOA $(\hat{\theta}, \hat{\phi})$ can be used to estimate the satellite attitude.

The second simulation investigates the influences of the number of snapshots and the input SNR on performance. The precision of the DOA $(\hat{\theta}, \hat{\phi})$ and the attitude determination can be described with the average root mean square error (RMSE) of estimates from 200 Monte Carlo trials

$$\mathrm{RMSE} = \sqrt{\frac{1}{200J}\sum_{i=1}^{200}\sum_{j=1}^{J}\left(x_j^{\mathrm{true}} - \hat{x}_j^i\right)^2} \tag{34}$$

where J is the total step number in each trial; x_j^{true} is the actual value; and $\hat{x}_j^i$ is the estimation of x_j^{true} in the ith Monte Carlo trial. The RMSEs of the DOA estimation and the attitude determination versus the input SNR with $L = 100$ are shown in Table 1. The RMSEs of the DOA estimation and the attitude determination versus the number of snapshots with an SNR of 0 dB are shown in Table 2.

Obviously as shown in Tables 1 and 2, the DOA estimation is more accurate as the increases of the number of snapshots and the input SNR. It is consistent with the results in Section 4.2. In the same way, the performance of the attitude determination is much better. Especially, the RMSE of the attitude determination is better than 0.1° when the input SNR is greater than −6 dB or the number of snapshots is more than 50.

In addition, we can see that the attitude determination accuracy is higher than that of the DOA estimation especially in the case of lower input SNRs and less number of snapshots in Tables 1 and 2 (e.g., the case of one snapshot or −10 dB). The error of the DOA estimation $\boldsymbol{W}$ is injected into the attitude measurement equation Eq. (18) and its statistical properties are analyzed in Section 4.2. As a result of the attitude determination using the measurements as well as a prior knowledge about the time evolution of attitude and the statistical properties of the measurement error $\boldsymbol{W}$, the precision of the attitude determination is improved. The simulation results also demonstrate the validity of the measurement error $\boldsymbol{W}$ analysis in Section 4.2.

To sum up, the proposed method of attitude determination using DOAs estimation of ground terminals or stations could be an available method for communication satellites with smart antennas. Its accuracy depends on the input SNR and the number of snapshots. Thus, the above factors should be comprehensively considered for different situations in practical applications.

7. Conclusions and future work

This paper introduces a novel approach to determine satellite attitude with DOA estimation. Based on the geometrical relationship between a signal source (a ground station or a ground mobile user) and an antenna array, an attitude measurement equation is derived and the error of the attitude measurement equation is analyzed in detail. By using this equation, the algorithm of attitude determination is obtained for communication satellites with smart antennas. Simulation results validate that this algorithm can estimate the attitude of a satellite effectively. The method could be a backup method of attitude determination to prevent a system failure. In addition, the influences of the SNR and the number of snapshots are explored on the performance of attitude determination.

For future studies, on conditions of several reference sources on the Earth for attitude determination and DOA estimation in presence of mutual coupling, the effects of attitude accuracy will be discussed in great detail in another paper.

Acknowledgements

This study was co-supported by the National Natural Science Foundation of China (No. 61073012) and the Aeronautical Science Foundation of China (No. 20111951015).

References

1. Garrison TP, Ince M, Pizzicardi J, Swan PA. Systems engineering trades for IRIDIUM constellation. *AIAA J Spacecraft Rockets* 1997;**34**(5):675–80.
2. Lin LX. Globalstar constellation and its attitude and orbit control technology. *Aerospace China* 1997;**1**:17–21 [Chinese].
3. Dybdal RB, SooHoo KM. Narrow beamwidth satellite antenna pointing and tracking. In: *2011 IEEE international symposium antennas propagation (APSURSI)*, 2011 July 3–8; El Segundo, CA, USA; 2011. p. 2012–5.
4. Yang M, Wang H, Wu CJ, Wang CH, Ding LC, Zheng YM, et al. Space flight validation of design and engineering of the ZDPS-1A pico-satellite. *Chin J Aeronaut* 2012;**25**(5):725–38.
5. Liu HY, Wang HN. Application of mean field annealing algorithms to GPS-based attitude determination. *Chin J Aeronaut* 2004;**17**(3):165–9.
6. Wang JQ, Xiong K, Zhou HY. Low-frequency periodic error identification and compensation for star tracker attitude measurement. *Chin J Aeronaut* 2012;**25**(5):615–21.
7. Ousmane OA, Ming FS, Tariq PS. Comparison between MUSIC and ESPRIT direction of arrival estimation algorithms for wireless communication systems. In: *2012 International conference on future generation communication technology (FGCT)*, 2012 Dec 12–14; London, UK; 2012. p. 99–103.
8. Liu Y, Wu SJ, Wu MY, Li CM, Zhang HG. Wideband DOA estimation based on spatial sparseness. *Acta Aeronaut Astronaut Sin* 2012;**33**(11):2028–38 [Chinese].
9. Dandekar KR, Ling H, Xu GH. Experimental study of mutual coupling compensation in smart antenna applications. *IEEE Trans Wireless Commun* 2002;**1**(3):480–7.
10. Tabrikian J, Shavit R, Rahamim D. An efficient vector sensor configuration for source localization. *IEEE Signal Process Lett* 2004;**11**(8):609–93.
11. He J, Swamy MNS, Ahmad MO. Joint DOA and DOA estimation for MIMO array with velocity receive sensors. *IEEE Signal Process Lett* 2011;**18**(7):399–402.
12. Ishiguro K, Yamada T, Araki S, Nakatani T, Sawada H. Probabilistic speaker diarization with bag-of-words representations of speaker angle information. *IEEE Trans Audio Speech Lang Process* 2012;**20**(2):447–60.
13. He M, Chen GD, Zhang K. Aircraft attitude/heading estimation using a dipole triad antenna. *J Radars* 2012;**2**(6):157–62 [Chinese].
14. Gupta L, Singh RP. Array signal processing: DOA estimation for missing sensors. In: *2010 International conference power, control and embedded systems (ICPCES)*, 2010 Nov 29-Dec 1; Allahabad, India; 2010. p. 1–4.
15. Whitelonis N, Ling H. High-resolution radar imaging through a pipe via MUSIC and compressed sensing. *IEEE Trans Antennas Propag* 2013;**61**(6):3252–60.
16. Liao B, Zhang ZG, Chan SC. DOA estimation and tracking of ULAs with mutual coupling. *IEEE Trans Aerosp Electron Syst* 2011;**48**(1):891–904.
17. Niow CH, Hui HT. Improved noise modeling with mutual coupling in receiving antenna arrays for direction-of-arrival estimation. *IEEE Trans Wireless Commun* 2012;**11**(4):1616–21.
18. Yang B, Xu GH, Jin J, Zhou Y. Comparison on EKF and UKF for geomagnetic attitude estimation of LEO satellites. *Chin Space Sci Technol* 2012;**32**(6):23–30 [Chinese].
19. Julier S, Uhlmann J, Durrant-Whyte HF. A new method for the nonlinear transformation of means and covariance in filters and estimators. *IEEE Trans Autom Control* 2000;**45**(3):477–82.
20. Han K, Wang H, TU BJ, Jin ZH. Pico-satellite autonomous navigation with magnetometer and sun sensor data. *Chin J Aeronaut* 2011;**24**(1):46–54.

Yang Bin is a Ph.D. student in the School of Electronic and Information Engineering at Beihang University. He received his B.S. and M.S. degrees in signal and information processing from North University of China in 2003 and 2007, respectively. His main research interests are statistical signal processing and multi-antenna communications.

He Feng is a lecturer in the School of Electronics and Information Engineering at Beihang University in China. He received his PhD degree in Communication and Information System in March 2009. His research interests cover airborne communication, real-time system, and distributed computing.

Jin Jin received his B.S. and Ph.D. degrees in Navigation, Guidance, and Control from Beijing Institute of Technology in 2006 and 2011, respectively, and then became a postdoctor at Tsinghua University till now. His main research interests are spacecraft attitude dynamics and control, aerospace engineering.

Xiong Huagang is a full professor in the School of Electronics and Information Engineering at Beihang University in China. His research interests include digital communication and avionics system.

Xu Guanghan is a professor and Ph.D. advisor in the School of Electronics and Information Engineering at Beihang University in China. He received his Ph.D. degree from Stanford University in 1991. His current research interests are array signal processing and multi-antenna communication.